Journal of Alloys and Compounds. Vol. 478. 2009. Pag. 19-21

http://dx.doi.org/10.1016/j.jallcom.2008.11.072

Specific heat measurements on amorphous and nanocrystalline Al88Y5Ni5Co2

J. S. Blázquez[a], M. Millán[a], C. F. Conde[a], A. Conde[a*], J. Latuch[b], T. Kulik[b]

[a] *Dpto. Física de la Materia Condensada, ICMSE-CSIC, Universidad de Sevilla, P.O. Box 1065, 41080, Sevilla, Spain*

[b] *Faculty of Materials Science and Engineering, Warsaw University of Technology, ul. Woloska 141, 02-507, Warsaw, Poland.*

Abstract

Specific heat at constant pressure, C_P, was measured on amorphous and nanocrystalline $Al_{88}Y_5Ni_5Co_2$ alloys from differential scanning calorimetry experiments. Linear behavior of C_P versus temperature from 323 to 423 K is explained by conduction electrons contribution and dilatation correction factor. Results indicate that the Fermi energy increases as nanocrystallization progresses, although the estimated values are clearly lower than that found for crystalline Al.

PACS codes: 61.46.Hk; 65.40.Ba.

Keywords: Specific heat; nanocrystalline alloys

* Prof. A. Conde:

Tel: (34) 95 455 28 85, Fax: (34) 95 461 20 97, e-mail: conde@us.es

Journal of Alloys and Compounds. Vol. 478. 2009. Pag. 19-21

http://dx.doi.org/10.1016/j.jallcom.2008.11.072

1. Introduction

The study of amorphous and nanocrystalline alloys has been a field of intense research and applicability since the pioneer work of Duwez [1] as their particular characteristics lead to innovative properties and behaviors which, sometimes, overcome those of the corresponding stable structures. Among these systems, Fe-based [2] and Al-based alloys [3] are particularly interesting for their outstanding soft magnetic and mechanical properties, respectively.

Several properties are severely affected by the existence of an amorphous or nanocrystalline microstructure implying a high fraction of atoms located at surfaces. Among them, specific heat is observed to differ from that of the corresponding crystalline microstructure [4,5,6,7]. Previous studies on Fe-based ferromagnetic nanocrystalline alloys [8] showed that the magnetic contribution due to the Curie transition of the amorphous matrix jeopardizes the effect of nanocrystalline microstructure on the specific heat through the conduction electron contributions and the bulk modulus. In this study, a non-magnetic Al-based alloy has been chosen to overcome this difficulty and specific heat measurements on amorphous and several nanocrystalline samples have been systematically studied.

2. Experimental

Amorphous ribbons of $Al_{88}Y_5Ni_5Co_2$ composition were produced by melt-spinning technique. Microstructure of the samples was studied from X-ray diffraction (XRD) using Cu-kα wavelength. Differential scanning calorimetry (DSC) in a Perkin-

Journal of Alloys and Compounds. Vol. 478. 2009. Pag. 19-21

http://dx.doi.org/10.1016/j.jallcom.2008.11.072

Elmer DSC7 was used to characterize the devitrification process of amorphous as-cast samples as well as to measure the specific heat at constant pressure, C_P, of samples with different crystalline fraction following the procedure described elsewhere [9].Three scans obtained in the same conditions and without significant delay (in order to minimize errors derived from baseline drift) are needed for each measurements: a baseline obtained with an empty pan, a scan obtained with a sapphire standard sample for which the value of specific heat is known in all the studied range and, finally, this scan is repeated for the sample of interest.

3. Results

Figure 1 shows the DSC scan obtained at 20 K/min of an as-cast amorphous sample. The devitrification process occurs in several stages. The former process (peak temperature, T_P=461 K) corresponds to the formation of almost pure α-Al nanocrystals embedded in a residual amorphous matrix enriched in Y, Ni and Co [3,10,11] as it is shown in figure 2. Several exothermic events are detected at higher temperatures: T_P=613, 641 and 646 K, respectively. These events might correspond to the formation of intermetallic phases (Al_3Ni, Al_3Y and Al_9Co_2) as reported in the literature [3,10,11,12].

In order to study the effect of nanocrystallization on the specific heat, nanocrystalline samples with different amount of nanocrystals were produced by heating as-cast samples up to different temperatures at 20 K/min. The nanocrystalline

Journal of Alloys and Compounds. Vol. 478. 2009. Pag. 19-21

http://dx.doi.org/10.1016/j.jallcom.2008.11.072

fraction, X, was calculated as the ratio $X=H(T_h)/H_{nano}$, where $H(T_h)$ is the enthalpy integrated from the crystallization onset to the maximum temperature achieved during the heating treatment, T_h, and H_{nano} is the total enthalpy area of the nanocrystallization process. It is worth mentioning that the value X=1 does not correspond to a fully crystalline sample but to a nanocrystalline sample with the maximum fraction of α-Al nanocrystals.

Figure 3 shows an example of the C_P plots obtained as a function of temperature for the different samples studied. Independently of the nanocrystalline fraction, the behavior of C_P can be fitted to a linear trend in the temperature range studied. This yields two different parameters, the intercept by extrapolating to T=0 K, C_p^0, and the slope, m. Figure 4 shows the slope as a function of the nanocrystalline fraction, which decreases as X increases. The Y-axis error bars shown (Δm) were obtained from the minimum square linear fitting of the data. This error does not consider systematic errors of C_P measurements which would shift vertically the whole C_P curve as those arising from the measurement of the mass (~5 %). These errors do not affect the slope but are evidenced in the dispersion data of the intercept, where no trend is observed and leading to an average value, $<C_P^0>$=1030±50 J kg^{-1} K^{-1}. The X-error bars, ΔX, were derived from:

$$\Delta X = \frac{1}{H_{nano}\beta}\frac{dH}{dt}\Delta T \qquad (1)$$

where β is the heating rate, dH/dt is the heat flow registered by the DSC and ΔT is the experimental error of the temperature in the equipment, which could be considered as ≤1 K.

Journal of Alloys and Compounds. Vol. 478. 2009. Pag. 19-21

http://dx.doi.org/10.1016/j.jallcom.2008.11.072

4. Discussion

In the studied case, the specific heat at constant pressure can be linked with the specific heat at constant volume as [13]:

$$C_P = C_V + C_D = C_{VH} + C_{VA} + C_{VV} + C_{VE} + C_D \quad (2)$$

where C_D is the dilatation correction, C_{VH} corresponds to the harmonic vibrations contribution, C_{VA} corresponds to the anharmonic vibrations corrections not considered in C_D, C_{VV} to the equilibrium vacancies in the lattice and C_{VE} corresponds to conducting electrons contributions.

The Debye temperature of the studied alloy is expected to be θ_D~250 K in agreement with data reported in the literature for very similar compositions [14]. This fact allows us to approximate C_{VH} to the Dulong-Petit limit $3R$, (in J mol^{-1} K^{-1} units) where R is the gas constant. For pure Al, this value is 924.5 J kg^{-1} K^{-1} and assuming an average atomic mass of 32.30 mg for the studied alloys, it would decrease down to 772.2 J kg^{-1} K^{-1}.

In order to prevent further microstructural transformation on the studied samples during measurement, the temperature range explored in this study is below the crystallization onset temperature (~441 K) and, therefore, well below the melting point of the alloy. Hence C_{VA} and C_{VV} contributions could be considered as a very small correction to C_{VH}. In the case of C_{VA}, anharmonic corrections of higher order than C_D are negligible below T~3θ_D [15], ~750 K for the studied alloy. In the case of C_{VV}, its value per mol can be estimated as:

Journal of Alloys and Compounds. Vol. 478. 2009. Pag. 19-21

http://dx.doi.org/10.1016/j.jallcom.2008.11.072

$$C_{VV} = N_A \frac{< E_V >^2}{k_B T^2} \exp\left(- \frac{< E_V >}{k_B T} \right) = n_V \frac{< E_V >^2}{k_B T^2} \quad (3)$$

where N_A is the Avogadro number, $<E_V>$ is an average energy for the formation of a vacancy in the system, k_B is the Boltzamann constant and n_V is the vacancy population per mol. Considering for $< E_V >$ the value of vacancy formation in pure Al, $<E_V>$=0.66 eV [16], $C_{VV} \leq 3.3 \cdot 10^{-5}$ J mol^{-1} K^{-1}= $1.2 \cdot 10^{-3}$ J kg^{-1} K^{-1} (considering the atomic mass of Al) in the explored thermal range. This value is well below the contributions considered in this study ~10^2 J kg^{-1} K^{-1}.

After these contributions are neglected, the value of C_V is:

$$C_P = C_{VH} + C_{VE} + C_D \quad (4)$$

The linear increase with the temperature observed in figure 3 for all the studied samples can be ascribed to both C_D and C_{VE} contributions and therefore, the obtained value of $<C_P^0>$=1030±50 J kg^{-1} K^{-1} might correspond to C_{VH}. In fact its value is in between the Dulong-Petit limit and the experimental value obtained for liquid Al [17].

In the case of the conduction electrons contribution, it is possible to link C_{VE} with the electric conductivity, σ, of the alloy through the Wiedemann-Franz law, which applicability has been widely tested in crystalline Al [18], liquid Al [17,19] and quasicrystals [20]. Wiedemann-Franz law assumes a proportionality of the ratio between the thermal and electrical conductivities and the temperature:

$$\frac{k}{\sigma} = L\,T \quad (5)$$

Journal of Alloys and Compounds. Vol. 478. 2009. Pag. 19-21

http://dx.doi.org/10.1016/j.jallcom.2008.11.072

where k is the thermal conductivity and L is the Lorentz constant. As the thermal conductivity is proportional to C_{VE} and it can be written:

$$\frac{C_{VE}}{T} = a\,\sigma = \frac{a}{\rho} \tag{6}$$

where $\rho=1/\sigma$ is the resistivity and a is a constant. The linear fitting of C_P curves implies an almost constant value of σ (and ρ) in the temperature range explored. In fact, it can be observed that $\rho(T)$ is almost constant in comparison with the changes observed for this magnitude with the nanocrystallization [21,22].

On the other hand, C_D, first order anharmonic correction to C_{VH}, can be expressed as [4]:

$$C_D = \frac{(\gamma\, C_{VH})^2}{B\,V}\,T \tag{7}$$

where γ is the Grüneissen parameter, B is the bulk modulus and V is the molar volume. All these parameters can be approximated to temperature independent values and the linear dependence of C_P is thus explained.

In order to explain the microstructural dependency of m, it is convenient to develop the expressions of B and C_{VE}, which, in the frame of free electrons theory, lead to:

$$C_D = \frac{(\gamma\, C_{VH})^2}{\frac{2}{3}\,n\,\varepsilon_F\,V}\,T \tag{8}$$

Journal of Alloys and Compounds. Vol. 478. 2009. Pag. 19-21

http://dx.doi.org/10.1016/j.jallcom.2008.11.072

$$C_{VE} = \frac{\pi^2 n\, k_B^{\,2}}{2\,\varepsilon_F} T \qquad (9)$$

where n is the number density of electrons and ε_F is the Fermi energy. From expression (6) and (7) it is observed that the slope m is proportional to $1/\varepsilon_F$. If the decrease of m as X increases is ascribed to changes in ε_F, it would involve an almost linear increase of ε_F with the nanocrystalline fraction X. This is in agreement with the reported values of ε_F for amorphous Al-based alloys [23] and the behavior of the thermoelectric power with the crystallization [23,24].

Using the experimental values of B, Fermi temperature ($T_F=\varepsilon_F/k_B$) and C_{VE}/T for pure Al (76 GPa, $13.6\cdot10^4$ K and 0.046 J kg^{-1} K^{-2}, respectively [18]) and comparing with the obtained value of m in this study a rough estimation of $T_F\sim10^4$ K is obtained for the amorphous $Al_{88}Y_5Ni_5Co_2$ alloy and double value for the nanocrystalline alloy with X=1. These values are of the order of that found for $Al_{88}Sm_8Ni_4$ estimated from thermoelectric power measurements. The decrease of the Fermi energy of amorphous and nanocrystalline alloys with respect to crystalline alloys implies a decrease of the bulk modulus and could be qualitatively explained in the frame of excess volume model developed by Wagner [4].

Conclusions

Specific heat at constant pressure, C_P, was obtained on amorphous and nanocrystalline $Al_{88}Y_5Ni_5Co_2$ alloys from differential scanning calorimetry experiments

Journal of Alloys and Compounds. Vol. 478. 2009. Pag. 19-21

http://dx.doi.org/10.1016/j.jallcom.2008.11.072

from 323 to 423 K. Linear behavior of C_P versus temperature in the studied range is explained by conduction electrons contribution and dilatation correction factor.

The slope of C_P curves is clearly larger for all the studied samples than that of crystalline Al and decreases as nanocrystallization progresses. This indicates a lower value of Fermi energy for the amorphous alloy, which increases as nanocrystallization progresses.

Acknowledgements

This work was supported by MEC of the Spanish Government and EU FEDER (Project MAT2007-65227), the PAI of the Regional Government of Andalucía (Project P06-FQM-01823). J.S.B. acknowledges a research contract from this Regional Government.

Journal of Alloys and Compounds. Vol. 478. 2009. Pag. 19-21

http://dx.doi.org/10.1016/j.jallcom.2008.11.072

References

[1] W. Klement Jr., R.H. Willens, P. Duwez, Nature 187 (1960) 869.,
[2] M. E. McHenry, M. A. Willard, D. E. Laughlin, Prog. Mat. Sci. 44 (1999) 291-433.
[3] A. Inoue, Prog. Mat. Sci. 43 (1998) 365-520.
[4] M. Wagner, Phys. Rev. B 45 (1992) 635-639.
[5] L. Wang, Z. Tan, S. Meng, A. Druzhinina, R. A. Varushchenko, G. Li, J. Non-Cryst. Sol. 296 (2001) 139-142.
[6] G. Kh. Panova, N. A. Chernoplekov, A. A. Shikov, T. Kemeny, L. F. Kiss, Phys. Solid State 49 (2007) 1617-1622.
[7] I. Avramov, M. Michailov, J. Phys.: Cond. Matter 20 (2008) 295224.1-4.
[8] J.S. Blázquez, M. Millán, C. F. Conde, V. Franco, A. Conde, A. Lozano-Pérez, J. Non-Cryst. Solids doi:10.1016/j.jnoncrysol.2008.05.075
[9] Perkin-Elmer DSC2 Operation Instructions (1981) Norwalk, Connecticut, U.S.A. p. 3-20.
[10]J.S. Blázquez, E. Fazakas, H. Dimitrov, J. Latuch, L. Varga, T. Kulik, J. Non-Cryst. Solids 351 (2005) 158-166.
[11] J. Latuch, H. Matyja, V. I. Fadeeva, Mater. Sci. Eng. A 179-180 (1994) 506-510.
[12] A. Révész, L. K. Varga, S. Suriñach, M. D. Baró, J. Non-Cryst. Solids 343 (2004) 143-149.
[13] P. J. Meschter, J. W. Wright, C. R. Brooks, T. G. Kollie, J. Phys. Chem. Solids 42 (1981) 861-871.
[14] M. Yewondssen, R. A: Dunlap, D. J. Lloyd, J. Phys.: Cond. Matter. 4 (1992) 461-472.
[15] R. A. MacDonald, R. D. Mountain, Phys. Rev. B 20 (1979) 4012-4017.
[16] M.J. Gillan, J. Phys.: Condens. Matter 1 (1989) 689-711
[17] G. R. Gathers, Int. J. Thermophys. 4 (1983) 209-226.
[18] N. W. Ashcroft, N. D. Mermin, Solid State Physics, Holt, Rinehart and Winston, 1976, U.S.A.
[19] G. R. Gathers, Int. J. Thermophys. 4 (1983) 209-226.
[20] E. Maciá, Appl. Phys. Letters 81 (2002) 88-90.
[21] K. Pekala, P. Jaskiewicz, J. Latuch, A. Kokoszkiewicz, J. Non-Cryst. Solids 211 (1997) 72-76.
[22] K. L. Sahoo, A. K. Panda, S. Das, V. Rao, Mater. Letters 58 (2004) 316-320.
[23] K. Pekala, J. Non-Cryst. Solids 353 (2007) 888-892.
[24] K. Pekala, J. Non-Cryst. Solids 287 (2001) 183-186.

Journal of Alloys and Compounds. Vol. 478. 2009. Pag. 19-21

http://dx.doi.org/10.1016/j.jallcom.2008.11.072

Figure captions

Figure 1. DSC plot of as-cast simple at 20 K/min.

Figure 2. XRD spectrum for a sample heated up to 502 K, showing the nanocrystalline microstructure developed during the first DSC exothermic peak.

Figure 3. Specific heat at constant pressure versus temperature for a sample with X=0.3.

Figure 4. Slope obtained from the linear fitting of C_P versus T curves as a function of the DSC transformed fraction..

Journal of Alloys and Compounds. Vol. 478. 2009. Pag. 19-21

http://dx.doi.org/10.1016/j.jallcom.2008.11.072

Figure 1

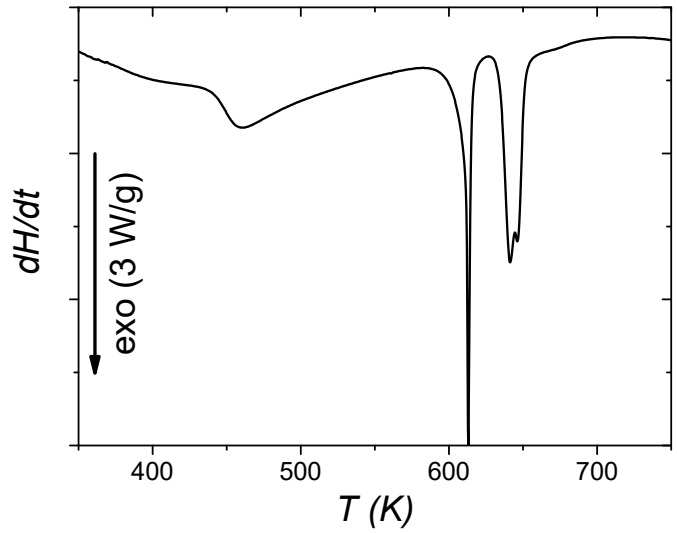

Journal of Alloys and Compounds. Vol. 478. 2009. Pag. 19-21

http://dx.doi.org/10.1016/j.jallcom.2008.11.072

Figure 2.

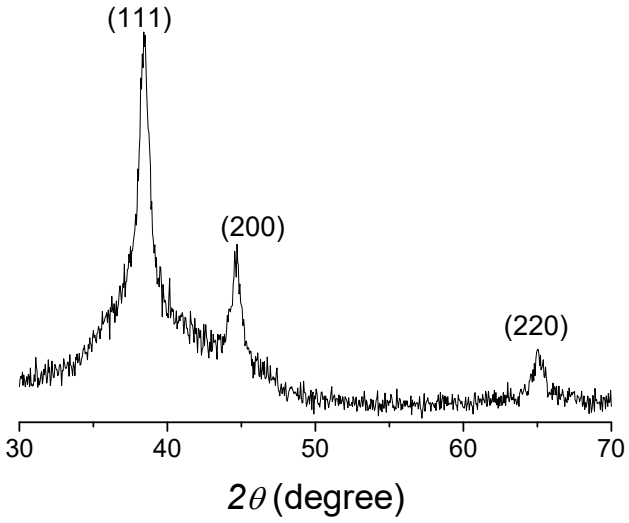

Journal of Alloys and Compounds. Vol. 478. 2009. Pag. 19-21

http://dx.doi.org/10.1016/j.jallcom.2008.11.072

Figure 3

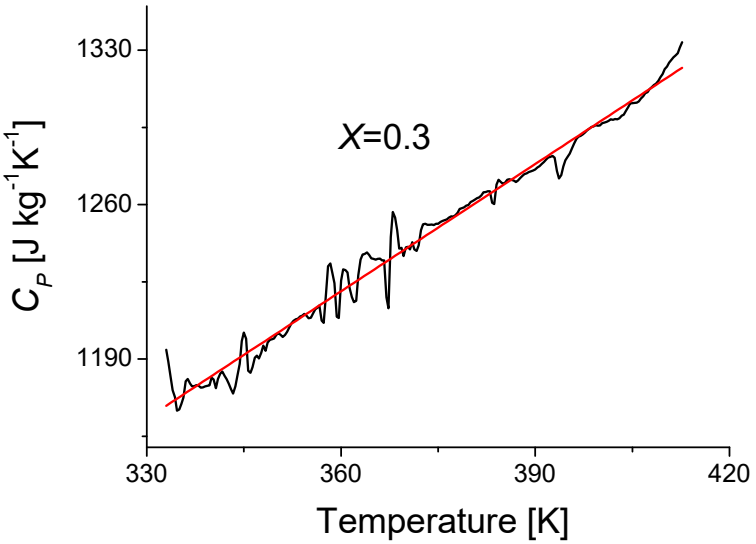

Journal of Alloys and Compounds. Vol. 478. 2009. Pag. 19-21

http://dx.doi.org/10.1016/j.jallcom.2008.11.072

Figure 4.